DOI: https://doi.org/10.37434/tpwj2025.08.03

OBTAINING FUNCTIONALLY-GRADED METAL-MATRIX MATERIALS Ti–6Al–4V + WC IN THE PROCESS OF 3D PRINTING BY THE METHOD OF ADDITIVE PLASMA-ARC DEPOSITION

V. Korzhyk[1], **A. Grynyuk**[2], **O. Babych**[2], **O. Berdnikova**[1], **Ye. Illiashenko**[1], **O. Bushma**[1]

[1]E.O. Paton Electric Welding Institute of the NASU
11 Kazymyr Malevych Str., 03150, Kyiv, Ukraine
[2]Scientific-Research Institute of Welding Technologies in Zhenjiang Province
233 Yonghui Road, Xiaoshan District, Hangzhou City, Zhejiang Province, China

ABSTRACT

The possibility of 3D printing by additive plasma-arc surfacing of three-dimensional products from composite functionally-graded metal-matrix materials, in which the matrix is the titanium alloy Ti–6Al–4V and the reinforcing phase is tungsten carbide, has been experimentally confirmed. The technology of additive plasma-arc deposition with simultaneous feeding of powder or filler wire of titanium alloy Ti–6Al–4V Grade 5 and spherical WC powder into the plasma arc allows obtaining three-dimensional samples from functionally-graded metal-matrix materials of the "wall" type, in which the content of tungsten carbide along their height varies from 0 to 50 vol.% with a corresponding change in the hardness index from *HRC* 32 for the lower (deep) layers and up to *HRC* 56–66 and higher towards the surface layers. By selecting plasma spraying modes and energy input, it is possible to change the hardness, microstructure, and microhardness of the matrix of the material of the deposited layers, including the degree of melting of spherical WC powder particles, namely, to preserve their spherical shape with a microhardness of *HV*0.1 = 2172–3796 or to achieve their partial and complete melting. In the case of preserving the spherical shape of WC particles in a matrix of titanium alloy Ti–6Al–4V, the presence of a metallurgical bond between them and this matrix is characteristic. It has been established that the tensile strength of the obtained materials for the case of additive deposition with Ti–6Al–4V filler wire with the addition of WC powder up to 50 vol.% reaches σ_t = 666.8 MPa, which corresponds to 75 % of the tensile strength of the Ti–6Al–4VBT6 Grade 5 alloy of identical chemical composition (annealed sheet), which acts as the matrix of the studied composite material. The impact strength of the samples of wall-type joints with welded layers of the composite material Ti–6Al–4V Grade 5 alloy + WC powder reaches up to 70–80 % of the level of this parameter of the Ti–6Al–4V Grade 5 titanium alloy sheet.

KEYWORDS: 3D printing, additive plasma-arc deposition, titanium alloys, tungsten carbide, functionally-graded materials, structure, mechanical properties

INTRODUCTION

In modern additive manufacturing two approaches are predominantly used to make a finished metal product [1–18]: layer-by-layer selective melting of the powder or direct growing of the part wall from the material in the powder or wire form. The energy of the laser (SLM) or electron beam (EBSM) is used for the processes of selective melting of the powder. Both these processes ensure forming parts according to the dimensions specified in the models. After 3D printing by these methods no machining of the part surface is used in most cases. These processes, however, have a number of disadvantages, namely: limited part dimensions, need to use fine powders (predominantly, 20–63, 20–105 μm) with a high coefficient of sphericity; need to use several times greater amount of the powder than the finished part volume, when growing a part with gradient differences in the mechanical properties at successive application of powders of different chemical composition, their mixing beyond the fusion zone occurs, which causes the need for rejection of the powder, remaining in the unit after printing is over.

Among additive technologies, using the deposition methods, the Wire Direct Energy Deposition/Wire Arc Additive Manufacturuing/3D Metal Printing (DED-W/WAAM/3DMP) or WAAM processes became the most widely accepted. They include the arc processes with application of nonconsumable or consumable electrode, as well as processes with short-circuiting of the arc gap (of Cold Metal Transfer (CMT) type) [19–20]. Particular attention is given to Plasma Metal Deposition (PMD) or additive plasma-arc deposition (APAD), which uses the energy of the plasma arc and has considerable potential, both in terms of realization of wide technological capabilities, and producing new materials during 3D printing [20].

It is necessary to note the following advantages and wider technological capabilities of PMD, compared to WAAM methods [20]:

- broad adjustment of the 3D printing productivity (from 0.02 up to 25 kg/h) and degree of detalization of volumetric elements (from 2.0–2.5 up to 10–20 mm

wide) through realization of the process, both in the mode of microplasma deposition with a low-current plasma arc (at currents of 5–35 A), and at currents of 50–450 A and higher (depending on the power of the welding current power source of plasma deposition unit);

● large range of adjustment of the energy input, heating zone and depth of penetration of the layers previously deposited by APAD, using transferred or non-transferred arc;

● 3D printing at straight and reverse polarity current, alternating current, including realization of the process of cathodic cleaning and destruction of the oxide films, at surfacing of light metal and alloys with high-melting oxide films on their surface;

● 3D printing using from one to four filler wires, including those with current-conducting wire with preheating;

● using solid and composite (flux-cored) wires, powders of light alloys and refractory metals, composite powders and mechanical mixtures of powders of alloys, metal ceramics, carbides, borides, etc., as filler material for 3D printing;

● realization of the process of 3D printing using a filler, which does not move together with the plasmatron during the layer deposition (metal grit, foil, thin metal strips), which is applied alternately after deposition of each layer (process, similar to "lamination" or selective melting);

● possibility of igniting the plasma arc without adding wire or powder, which allows conducting preheating of the base or deposited layers before additive deposition.

THE OBJECTIVE OF THE WORK

is confirmation of the possibility of additive plasma-arc deposition to produce during 3D printing spatial products from functionally-graded metal-matrix materials, where the metal matrix contains reinforcing grains of refractory compounds (carbides, borides, etc.) of a variable composition.

To achieve this objective it is necessary to:

● using additive plasma-arc deposition with simultaneous feeding into the plasma arc of powder or filler wire from titanium alloy Ti–6Al–4V Grade 5 and spherical WC powder, produce composite functionally-graded materials, where the matrix is titanium alloy Ti–6Al–4V, and tungsten carbide is the reinforcing phase of a varying content;

● study the structure of the produced composite materials and the possibility of controlling the degree of melting of spherical particles of tungsten carbide in the titanium alloy matrix;

● determine the main physical and mechanical properties of the produced Ti–6Al–4V+WC composite materials, compared with the characteristics of Ti–6Al–4V matrix alloy.

RESEARCH MATERIALS AND METHODS

Experiments were performed in the equipment developed in cooperation by PWI and RPC PLASER Ltd (Ukraine) [20] (Figure 1, *a*, *b*). In order to conduct the research, 3D products of "wall" type of the dimensions from 8×4 to 8×50 mm were made, using a specially developed all-purpose plasmatron (Figure 1, *c*), which allows realization of the process of additive deposition at simultaneous feeding of one or several powders, or simultaneous feeding of the powder and filler wire [20–23]. The possibility of producing a composite volumetric functionally-graded material of Ti–6Al–4V Grade 5 alloy + WC powder by realization of two technologies of additive plasma-arc deposition by: a) simultaneous feeding of dissimilar powders from two powder dispensers; b) addition of a mechanical mixture of powders from one feeder;

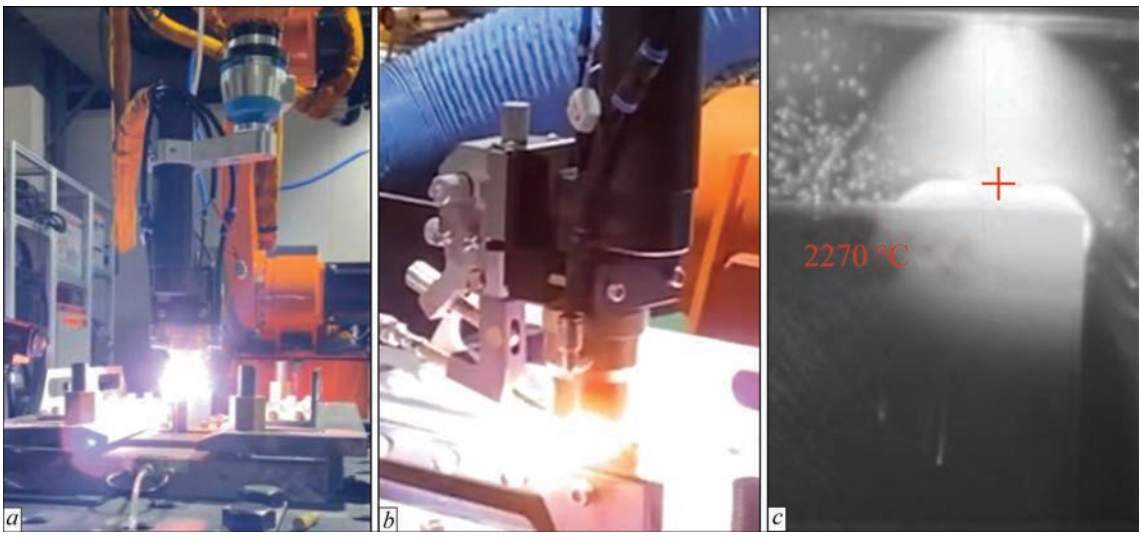

Figure 1. Robotic complex (*a*) and plasmatron (*b*), used to produce 3D samples of "wall" type and the process of plasma-arc deposition (*c*) of a single 2 mm layer during formation of the "wall" from a composite material with simultaneous feed of Ti–6Al–4V wire and spherical WC powder (*c*)

c) simultaneous feeding of a titanium alloy wire and tungsten carbide powder.

At the first stage of investigations plasma deposition was performed using a mixture of Ti–6Al–4V and WC powders. Owing to different density of the powders, the mechanical mixture started separating into individual components in the powder feeder hopper, and it was difficult to predict the presence of a specific amount of powder in the WC deposit.

In order to improve the stability of WC powder supply to the deposited metal, it was decided to either feed the WC and Ti–6Al–4V powder separately from different feeders, or feed the WC in the form of powder, and Ti–6Al–4V alloy in the form of wire. Considering that the coefficient of utilization of the material in the form of wire was higher than a similar coefficient in the powder, it was decided to feed the Ti–6Al–4V alloy in the form of wire. Wire 1.2 mm in diameter from Ti–6Al–4V titanium alloy was used, and the size of spherical particles of tungsten carbide was equal to 50–150 μm. Samples of "wall" type were grown during 3D printing on a substrate from 8 mm Ti–6Al–4V Grade 5 alloy. Deposition was performed on the end face of a sample 8 mm wide and 60 mm long.

Structural characteristics of the produced materials were studied using complex methods, which include measurement of hardness, microhardness, metallographic investigations of the structure, X-ray diffraction analysis and analysis of the chemical composition, using the procedure, described in [24–29]. Rockwell hardness (*HRC*) was measured in Laizhou Weiyi HRS-150S instrument, Vickers microhardness (*HV*) — in VH1102 instrument (USA) at 100 g load. Microstructural studies of the materials were conducted with application of a light microscope Zeiss Axio Imager M2m, and scanning electron microscope SEM-515 (Philips Company, Holland).

To determine the rupture strength of the deposited metal, 4 mm sheets from Ti–6Al–4V alloy were welded on a substrate from Ti–6Al–4V alloy. Sheets 4 mm thick were assembled with a guaranteed gap of 4 mm (Figure 2, *a*), in order to form a weld predominantly from filler material, namely Ti–6Al–4V titanium wire and WC powder. Here, the titanium wire feed rate

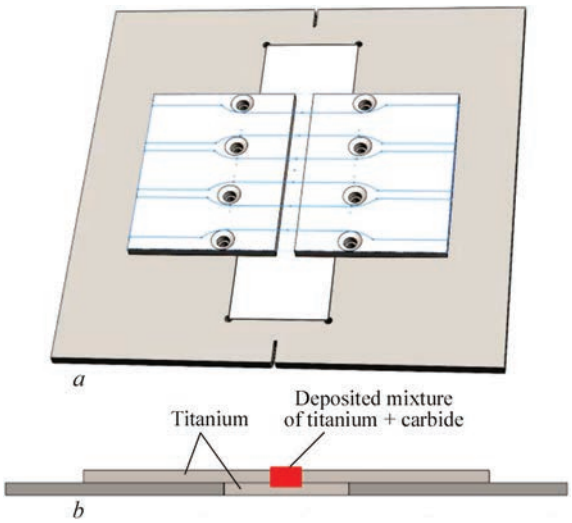

Figure 2. Schemes of sample layout when welding 4 mm sheets to determine the tensile strength of the weld metal

remained unchanged, but the amount of WC powder was changed, to ensure its content in the weld equal to 30 and 50 % of the total weld volume. Mechanical testing for ultimate strength and relative elongation of the studied samples with a deposits was conducted in an electronic universal Instron-5988 system. Size of samples for testing in keeping the standard was 12.5×3.22×128.5 mm, location of rupture was in the deposited material in all the samples. Samples for testing were cut out by spark cutting in the form of "spades" (Figure 2, *a*) with titanium at the edges and a strip of the deposited material in the middle, from material deposited into the gap between the two titanium plates (Figure 2, *b*). This allowed obtaining data on composite 3D samples of Ti–6Al–4V Grade 5 alloy + deposited layer + Ti–6Al–4V Grade 5 alloy.

Impact toughness testing of samples from the produced materials was conducted in Steel Research Nake NI300C system, using the methodology described in [29–32]. Dimensions of the test samples were as follows 10.0×10.0×55.0 mm. In order to measure the impact toughness of samples with a deposits, taking into account the zone of the deposited material fusion with the base, testing was conducted by two variants of the schemes: with application of the "frontal impact" (Figure 3, *a*) and "lateral impact" (Figure 3, *b*) with

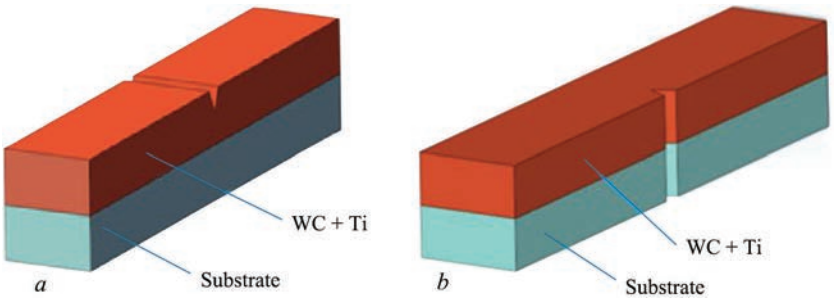

Figure 3. Schematic images of impact testing variants of samples with deposits: *a* — with application of "frontal impact"; *b* — "lateral impact"

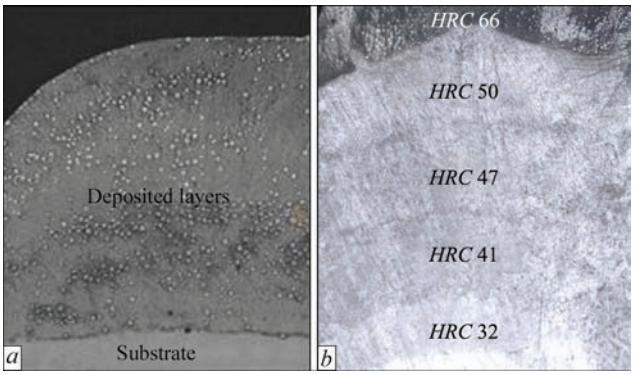

Figure 4. General view of the samples (*a*) and structure of a fragment of a sample (*b*, ×10) of "wall" type from a functionally-graded Ti–6Al–4V + WC material with WC content varying by sample height

a 2 mm deep notch. Test samples of 10 mm height were cut out, of which 5 mm are the substrate and 5 mm is the deposited layer. This allowed deriving data on two-layer samples of substrate + deposited layer, namely of Ti–6Al–4V alloy Grade 5 + deposited layer composite material.

INVESTIGATION RESULTS

The process of formation of a single layer 2 mm thick when manufacturing a 3D product of "wall" type with simultaneous feeding of Ti–6Al–4V wire and tungsten carbide is shown in Figure 1, *c*. Results of technological investigations enabled producing 3D products from Ti–6Al–4V + WC composite materials with adjustment of tungsten carbide content (Figure 4, *a*).

It is confirmed that the developed technology allows producing 3D multilayer material of gradient type and varying the content of tungsten carbide from 0 up to 50 % and, accordingly, the hardness by volume (height) from *HRC* 32 for the lower (deep-lying) layers from Ti–6Al–4V titanium alloy up to *HRC* 56–66 and higher towards the surface layers (Figure 4, *b*).

No pores or other defects were found in the material of the deposited layers of the produced samples. The fusion lines of the deposited layers are homogeneous (Figure 5, *a*). The line of fusion with the titanium substrate, on which samples of "wall" type were grown, is also homogeneous (Figure 5, *b*). For spherical WC particles with microhardness *HV*0.1 = 2172–3796, located in the matrix from Ti–6Al–4V titanium alloy, presence of a metallurgical bond with the matrix is characteristic, at their relatively uniform distribution in the material of this matrix (Figure 5, *c*, *d*).

Selection of plasma deposition modes and energy input allows varying the hardness, microstructure and microhardness of the matrix material of the deposited layers, including the degree of melting of spherical WC powder particles, namely reach their partial (Figure 6, *a*, *b*) or complete (Figure 6, *c*) melting.

So, for instance, partial melting of the carbide phase can be achieved along the WC/matrix interfac-

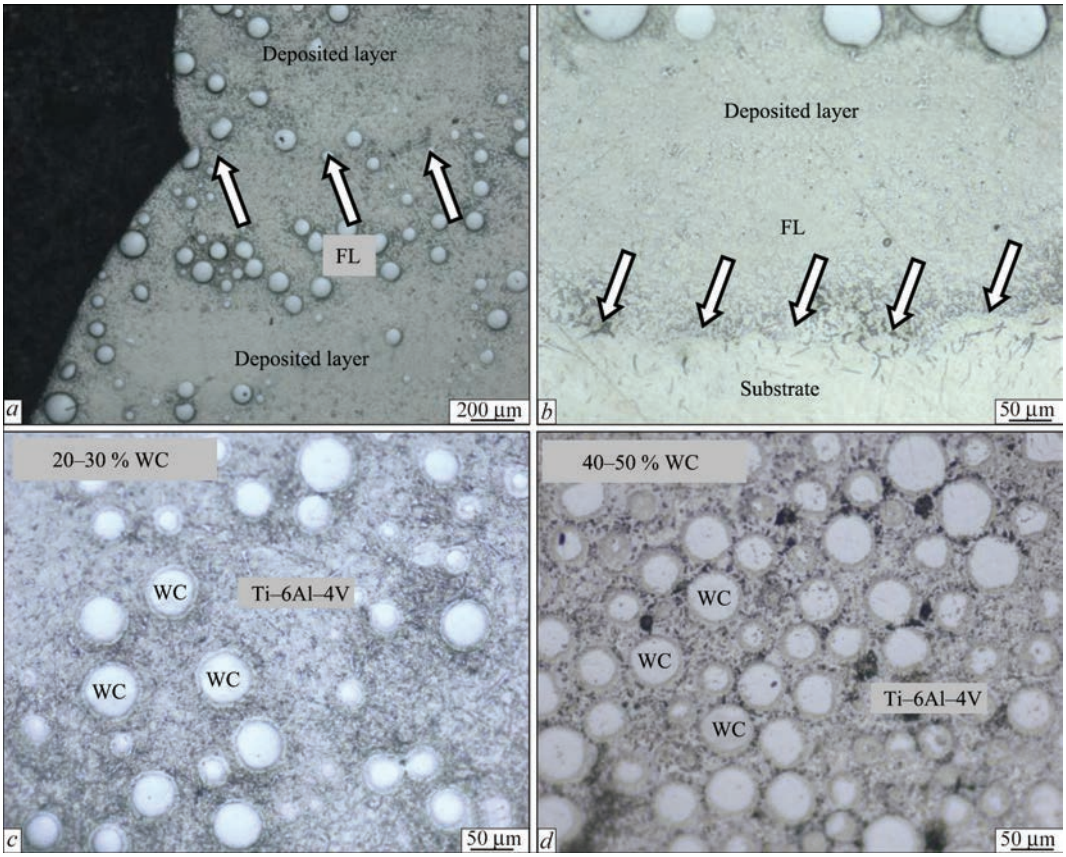

Figure 5. Microstructure of fragments of deposited layers in a sample of "wall" type from functionally-graded Ti–6Al–4V + WC material: *a*, *b* — fusion lines (FL); *c*, *d* — deposited layers with WC content varying by height (*a*, ×50; *c*–*e*, ×200)

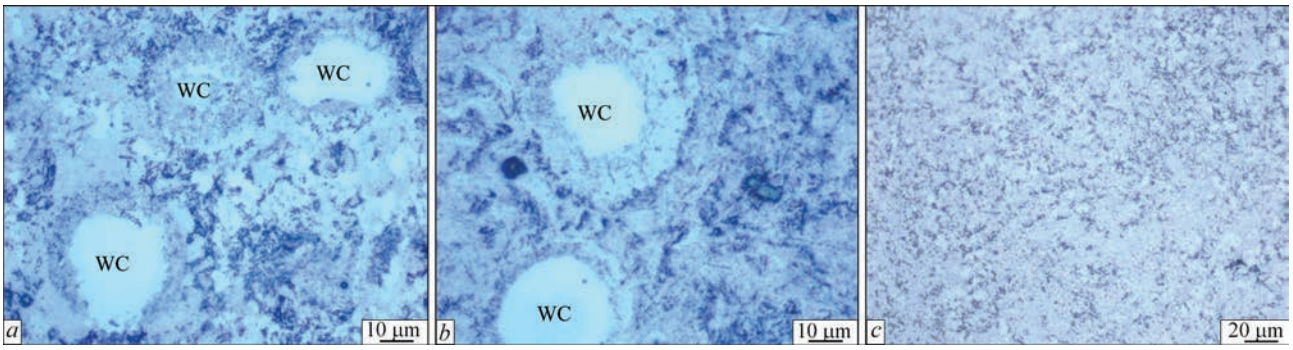

Figure 6. Microstructure of the material of Ti–6Al–4V + WC deposits

Table 1. Mechanical and structural parameters of the deposited layers: *n* is the number of the deposited layers; δ is the total thickness of the deposit; *HRC* is the maximal hardness from the deposit surface; *HV* is the cross-sectional microhardness; V_p is the maximal content of WC particles in the deposit material; σ_t is the rupture strength

No.	Deposited material type	*n*	δ, mm	*HRC*	*HV*0,1		V_p, %	σ_t, MPa
					Lower layer	Upper layer		
1	Ti–6Al–4V + WC powders	2	3.1	61	317.2–346.5	373.3–468.7	30	586.4
2		2	3.6	58	348.4–360.2	377.3–380.0	25	605.4
3	Ti–6Al–4V wire + WC powder	6	15	53	410.7–550.5	465.2–1187.4	40	611.4
4		2	8	66	479.4–859.0	706.0–1055.8	50	666.8
5		1	3.4	54.6	321.4–473.0	–	30	584.5
6		2	6.7	55.2	346.2–408.9	400.6–541.9	30	641.8

es in the deposited layers (Figure 6, *a*, *b*). In this case, the WC particles have already lost their spherical shape, and an interlayer enriched in tungsten and carbon is observed around them, where a new structure with a component of a stoichiometric composition of (W, Ti) C_x forms. Some WC particles have almost melted, but their initial WC particle/matrix interfaces are still observed (Figure 6, *a*). Some particles have dissolved completely. Their structure corresponds to that of the molten interlayers along the WC particle/matrix interfaces in the deposited layers (Figure 6, *c*).

For a more detailed analysis of physical and mechanical properties of the produced materials, several types of samples made by additive deposition using powder or wire from Ti–6Al–4V alloy with addition of WC powder during additive deposition we studied (Table 1).

Detailed analysis of the chemical composition of the deposit material confirmed the presence of WC powder solution (Table 2, Figure 7, *a*, local analysis Nos 1–6) in Ti–6Al–4V "matrix" and W content of up to 55 % (Table 2, Figure 7, *a*, *b*, fragments Nos 7, 8). It can be assumed that formation of exactly the dispersed particles of the carbide phases is observed in the volume of the deposited layer "matrix" (Figure 7, *b*).

X-ray phase analysis of the deposited layer material revealed the presence of the following phases: (α + β) — Ti; WC and WC + W_2C. It can be assumed that formation of W_2C carbide leads to additional strengthening of the deposit "matrix" material.

Mechanical rupture testing showed that the maximal values of σ_t = 641.8 and σ_t = 666.8 MPa are characteristic for samples Nos 6 and 4 (rupture point is the deposited material), with WC content of up to 30 and 50 %, respectively, which were produced by additive deposition, using Ti–6Al–4V filler wire with addition of WC powder (Table 1). Such strength values of the composite 3D samples of Ti–6Al–4V Grade 5 alloy + deposited layer + Ti–6Al–4V Grade 5 alloy correspond to 72–75 % of the ultimate strength of Ti–6Al–4VBT6 Grade 5 alloy (annealed sheet), identical in its chemical composition to the studied titanium alloy, acting as the matrix of the studied composite material [33–36]. In the deposited layers of sample No. 4 the volume fraction (V_p) of WC particles in the lower layer is equal to 50 %. The microstructure of the deposit upper layer is homogeneous with the microhardness of *HV* = 706.0–1055.8. In the upper zone of the deposit second layer WC particles are present in a small quantity. The lower layer microhardness is equal to *HV* = 479.4–859.0. Thus, at transition to from the lower layer into the upper one, *HV* increases by 30 % on average. The deposited material microstruc-

Table 2. Results of elemental analysis (wt.%) of the deposit material of sample No. 6 (Ti–6Al–4V wire + WC powder)

No.	1	2	3	4	5	6	7	8
Ti	23.7–21.3	37.1–39.4	53.4–68.9	43.5–79.2	44.7–59.1	50.9–70.7	57.8–68.3	44.9–51.3
W	76.4–78.7	60.6–62.9	31.1–46.6	20.8–56.5	40.9–55.3	29.3–49.5	31.7–42.23	48.7–55.1

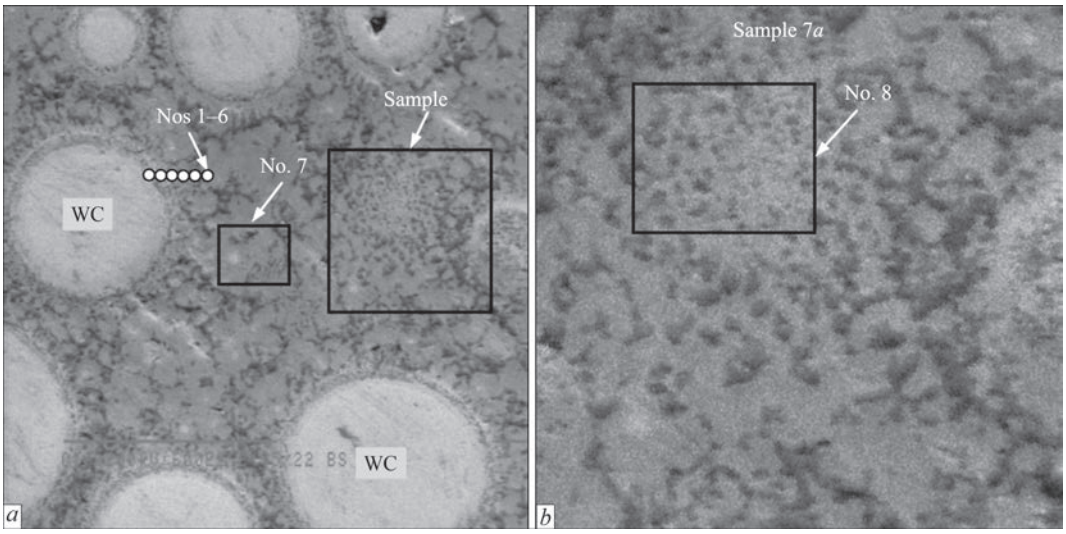

Figure 7. Material microstructure of the deposit of sample No. 6 (VT6 wire + WC powder), *a*×600; *b* — 10 times magnification of the fragment in Figure 7, *a*

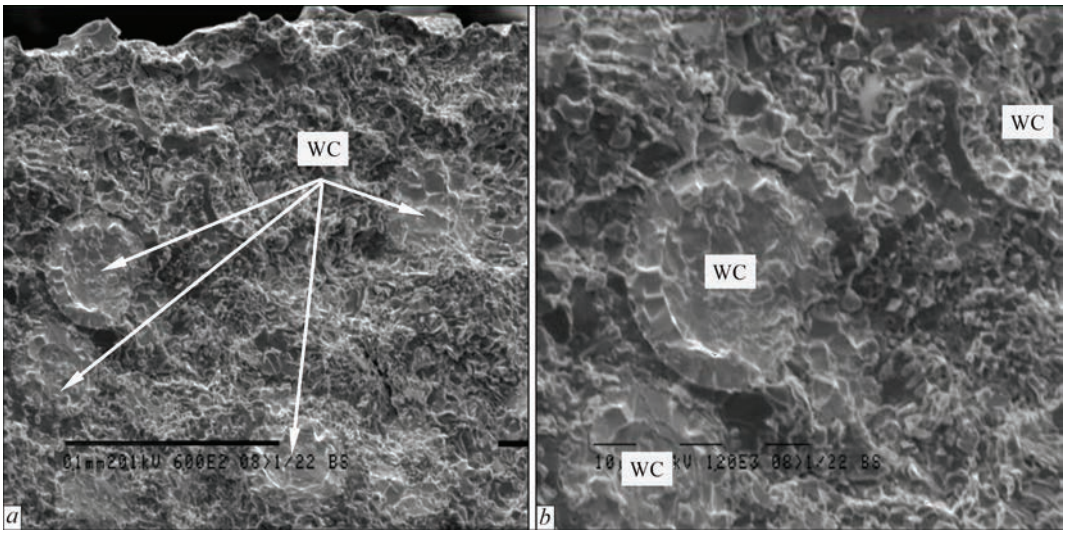

Figure 8. Fractograms of fracture surface of the deposit material of sample No. 6 (VT6 wire + WC powder) (*a*, ×600; *b*, ×1200)

ture in the two-layer sample No. 6 is characterized by 30 % volume fraction of WC particles at their even distribution in the first and second layers and gradient-free microhardness level (Table 1).

As a result of impact toughness tests of samples of "wall" type joints with deposited layers of Ti–6Al–4V Grade 5 alloy + WC powder composite material the following was established: this value is equal to 10.75–17.375 J/cm^2 for the studied samples with the content of tungsten carbide particles with the volume fraction of V_p = 30 % in the deposit material "matrix". The impact toughness value of Ti–6Al–4VBT6 Grade 5 alloy, used as the substrate for growing a wall from Ti–6Al–4V + WC material, is in the range of 19.5–21 J/cm^2. Thus, the 3D samples (10 mm in height, of which 5 mm is the substrate and 5 mm is the deposited layer) of different types of Ti–6Al–4V + WC composite material, produced by additive plasma deposition, are characterized by the overall impact toughness level, which can reach 70–80 % of that of this parameter for sheet Ti–6Al–4V Grade 5 the titanium alloy.

Fractographic studies of the fracture surface of the deposit material (BT6 wire+WC powder) revealed the following. Unmelted WC particles are characterized by brittle fracture (Figure 8).

The fracture mode of the deposit "matrix" material is predominantly mixed quasibrittle, with facet size of 3–8 μm and tough component with dispersed pits of 1–3 μm size. Such structural features of the microrelief of fracture surface of the deposit "matrix" are indicative of a set of high strength and toughness properties of the deposit material.

CONCLUSIONS

1. It was confirmed that the technology of plasma-arc additive deposition with simultaneous feeding of powder or filler wire of Ti–6Al–4V titanium alloy and spherical WC powder into the plasma arc allows producing 3D samples from functionally-graded met-

al-matrix materials, where the matrix is the titanium alloy with WC reinforcing phase. Such a technology realizes the possibility of varying the tungsten carbide content from 0 to 50 vol.% by the volume (sample height) and accordingly, change the hardness from *HRC* 32 for the lower (deep-lying) layers to *HRC* 56–66 and higher towards the surface layers.

2. Obtained materials are characterized by a defectfree structure, and the fusion lines of the deposited layers are homogeneous. By selecting the plasma deposition modes and energy input it is possible to change the hardness, microstructure and microhardness of the matrix of the deposited layer material, including the degree of melting of spherical WC powder particles, namely, preserve their spherical shape with microhardness *HV*0.1 = 2172–3796, or reach their partial or complete melting. In the case of preservation of the spherical shape of WC particles, present in the matrix from Ti–6Al–4V titanium alloy, a characteristic feature is preservation of the metallurgical bond with this matrix.

3. It was established that the ultimate strength of the produced materials reaches the value σ_t = 641.8–666.8 MPa (rupture location is in the deposited material), when testing the composite samples of the type of Ti–6Al–4V Grade 5 alloy+deposited layer + Ti–6Al–4V Grade 5 alloy for the case of additive deposition of Ti–6Al–4V filler wire with addition of WC powder up to 50 vol.%. This corresponds to 72–75 % of the ultimate strength of Ti–6Al–4VBT6 Grade 5 alloy (annealed sheet) of identical chemical composition, acting as the matrix of the deposited composite material. Impact toughness values of the composite material of Ti–6Al–4V Grade 5 alloy+deposited layer 10 mm in height, of which 5 mm is the substrate, and 5 mm is the deposited layer with 30 % volume fraction of WC particles in the "matrix" of the deposit material reaches up to 70–80 % of the level of this parameters for the sheet titanium alloy Ti–6Al–4V Grade 5.

REFERENCES

1. Zafar, F., Emadinia, O., Conceição, J. et al. (2023) A review on direct laser deposition of Inconel 625 and Inconel 625-based composites challenges and prospects. *Metals*, **13**, 787. DOI: https://doi.org/10.3390/met13040787
2. Preis, J., Wang, Z., Howard, J. et al. (2024) Effect of laser power and deposition sequence on microstructure of GRCop42 – Inconel 625 joints fabricated using laser directed energy deposition. *Materials and Design*, **241**, 112944. DOI: https://doi.org/10.1016/j.matdes.2024.112944
3. Zhukov, V., Grigorenko, G., Shapovalov V. (2016) Additive manufacturing of metal components (Review). *The Paton Welding J.*, **5–6**, 137–142. DOI: https:/doi.org/10.15407/tpwj2016.06.24
4. Su, G., Shi, Y. Li, G. et al. (2023) Improving the deposition efficiency and mechanical properties of additive manufactured Inconel 625 through hot wire laser metal deposition. *J. of Materials Processing Technology*, **322**, 118175. DOI: https://doi.org/10.1016/j.jmatprotec.2023.118175
5. Danielewski, H., Radek, N., Orman, L. et al. (2023) Laser metal deposition of Inconel 625 alloy — Comparison of powder and filler wire methods. *Materials Research Proceedings*, **34**, 154–160. DOI: https://doi.org/10.21741/9781644902691-19
6. Gu, Y., Xu, Y., Shi, Y. et al. (2022) Corrosion resistance of 316 stainless steel in a simulated pressurized water reactor improved by laser cladding with chromium. *Surface and Coatings Technology*, **441**, 128534. DOI: https://doi.org/10.1016/j.surfcoat.2022.128534
7. Ahn, D. (2021) Directed energy deposition (DED) process: State of the Art. *Int. J. of Precis. Eng. and Manuf.-Green Tech.*, **8**, 703–742. DOI: https://doi.org/10.1007/s40684-020-00302-7
8. Svetlizky, D., Das, M., Zheng, B. et al. (2021) Directed energy deposition (DED) additive manufacturing: Physical characteristics, defects, challenges and applications. *Materials Today*, **49**, 271–295. DOI: https://doi.org/10.1016/j.mattod.2021.03.020
9. King, W., Anderson, A., Ferencz, R. et al. (2015) Laser powder bed fusion additive manufacturing of metals; physics, computational, and materials challenges. *Applied Physics Reviews*, **2**, 041304. DOI: https://doi.org/10.1063/1.4937809
10. Hassila C., Paschalidou, M., Harlin, P. et al. (2022) Potential of nitrogen atomized alloy 625 in the powder bed fusion laser beam process. *Materials and Design*, **221**, 110928. DOI: https://doi.org/10.1016/j.matdes.2022.110928
11. Rehman, A., Karakas, B., Mahmood, M. et al. (2023) Additive manufacturing of Inconel-625: From powder production to bulk samples printing. *Rapid Prototyping J.*, 23(**9**), 1788–1799. DOI: https://doi.org/10.1108/RPJ-11-2022-0373
12. Chen, G., Zhao, S., Tan, P. et al. (2018) A comparative study of Ti–6Al–4V powders for additive manufacturing by gas atomization, plasma rotating electrode process and plasma atomization. *Powder Technology*, **333**, 38–46. DOI: https://doi.org/10.1016/j.powtec.2018.04.013
13. Yurtukan, E., Unal, R. (2022) Theoretical and experimental investigation of Ti alloy powder production using low-power plasma torches. *Transact. of Nonferrous Metals Society of China*, **32**, 175–191. DOI: https://doi.org/10.1016/S1003-6326(21)65786-2
14. Prokopov, V., Fialko, N., Sherenkovskaya, G. et al. (1993) Effect of the coating porosity on the processes of heat transfer under, gas-thermal atomization. *Powder Metall. Met. Ceram.*, **32**, 118–121. DOI: https://doi.org/10.1007/BF00560034
15. Yin, Z., Yu, D., Zhang, Q. et al. (2021) Experimental and numerical analysis of a reverse-polarity plasma torch for plasma atomization. *Plasma Chem. Plasma Process.*, **41**, 1471–1495. DOI: https://doi.org/10.1007/s11090-021-10181-8
16. Bobzina, K., Ernsta, F., Richardta, K. et al. (2008) Thermal spraying of cylinder bores wi-–4443. DOI: https://doi.org/10.1016/j.surfcoat.2008.04.023
17. Fan, H., Kovacevic, R. (2004)A unified model of transport phenomena in gas metal arc welding including electrode, arc plasma and molten pool. *J. Phys. D: Appl. Phys.*, **37**, 2531–2544. DOI: https://doi.org/10.1088/0022-3727/37/18/009
18. Sun, P., Fang, Z., Zhang, Y., Xia, Y. (2017) Review of the methods for the production of spherical Ti and Ti alloy powder. *JOM*, **69**, 1853–1860. DOI: https://doi.org/10.1007/s11837-017-2513-5
19. Korzhyk, V., Khaskin, V., Grynyuk, A. et al. (2021) Comparing features in metallurgical interaction when applying different techniques of arc and plasma surfacing of steel wire on titanium. *Eastern-European J. of Enterprise Technolo-*

gies, 112(**12**), 6–17. DOI: https://doi.org/10.15587/1729-4061.2021.238634
20. Korzhyk, V.M., Grynyuk, A.A., Khaskin, V.Yu. et al. (2023) Khuan Plasma-arc technologies of additive surfacing (3D printing) of spatial metal products: application experience and new opportunities. *The Paton Welding J*., **11**, 3–20. DOI: https://doi.org/10.37434/tpwj2023.11.01
21. Korzhik, V. (1992) Theoretical analysis of the conditions required for rendering metallic alloys amorphous during gas-thermal spraying. III. Transformations in the amorphous layer during the growth process of the coating. *Powder Metall. Met. Ceram*., 31(**11**), 943–948. DOI: https://doi.org/10.1007/BF00797621
22. Fialko, N., Prokopov, V., Meranova, N. et al. (1993) Thermal physics of gas thermal coatings formation processes. State of investigations. *Fizika i Khimiya Obrabotki Materialov*, **4**, 83–93.
23. Fialko, N., Prokopov, V., Meranova, N. et al. (1994) Temperature conditions of particle-substrate systems in a gas thermal deposition process. *Fizika i Khimiya Obrabotki Materialov*, **2**, 59–67.
24. Jing, H., Yu, Shi, Gang, Zh. et al. (2022) Minimizing defects and controlling the morphology of laser welded aluminium alloys using power modulation-based laser beam oscillation. *J. Manufacturing Processes*, **83**, 49–59. DOI: https://doi.org/10.1016/j.jmapro.2022.08.031
25. Fialko, N., Dinzhos, R., Sherenkovskii, J. (2021) Establishing patterns in the effect of temperature regime when manufacturing nanocomposites on their heat-conducting properties. *Eastern-European J. of Enterprise Technologies*, 4(**5–112**), 21–26. DOI: https://doi.org/10.15587/1729-4061.2021.236915
26. Li, X., Cui, L., Shonkwiler, S. et al. (2023) Automatic characterization of spherical metal powders by microscope image analysis: a parallel computing approach. *J. Iron Steel Res*., **30**, 2293–2300. DOI: https://doi.org/10.1007/s42243-022-00907-z
27. Appa Rao, G., Srinivas, M., Sarma, D. (2006) Effect of oxygen content of powder on microstructure and mechanical properties of hot isotatically pressed superalloy Inconel 718. *Materials Sci. and Eng. A*, 435(**3**), 84–99. DOI: https://doi.org/10.1016/j.msea.2006.07.053
28. Liu, Y., Zhang, S., Zhang, L. et al. (2024) Effects of oxygen content on microstructure and creep property of powder metallurgy superalloy. *Crystals*, 14(**4**), 358. DOI: https://doi.org/10.3390/cryst14040358
29. Kvasnytskyi, V., Korzhyk, V., Kvasnytskyi, V. et al. (2020). Designing brazing filler metal for heat-resistant alloys based on NI3AL intermetallide. *Eastern-European J. of Enterprise Technologies*, 12(**6**), 6–19. DOI: https://doi.org/10.15587/1729-4061.2020.217819
30. Skorokhod, A., Sviridova, I., Korzhik, V. (1994) Structural and mechanical properties of polyethylene terephthalate coatings as affected by mechanical pretreatment of powder in the course of preparation. *Mekhanika Kompozitnykh Materialov*, 30(**4**), 455–463.
31. Gu, Y., Zhang, W., Xu, Y. et al. (2022) Stress-assisted corrosion behaviour of Hastelloy N in FLiNaK molten salt environment. *NPJ Mater. Degrad*., **6**, 90. DOI: https://doi.org/10.1038/s41529-022-00300-x
32. Mao, D., Xie, Y., Meng, X. et al. (2024) Strength-ductility materials by engineering a coherent interface at incoherent precipitates *Materials Horizons*, 11(**14**), 3408–3419. DOI: https://doi.org/10.21203/rs.3.rs-3436553/v1
33. Ren, X.P., Li, H.Q., Guo H. et al. (2021) A comparative study on mechanical properties of Ti–6Al–4V alloy processed by additive manufacturing vs. traditional processing. *Materials Sci. and Eng.: A*, 817(**10**), 141384. DOI: https://doi.org/10.1016/j.msea.2021.141384
34. Mulay, R.P., Moore, J.A., Florando, J.N. et al. (2016) Microstructure and mechanical properties of Ti–6Al–4V: Mill-annealed versus direct metal laser melted alloys. *Materials Sci. and Eng*., 666(**1**), 43–47. DOI: https://doi.org/10.1016/j.msea.2016.04.012
35. Gargi Roya, Raj Narayan Hajraa, Woo Hyeok Kima et al. (2024) Microstructural evolution and mechanical properties of Ti–6Al–4V alloy through selective laser melting: Comprehensive study on the effect of hot isostatic pressing (HIP). *J. of Powder Materials*, 31(**1**), 1–7. DOI: https://doi.org/10.4150/KPMI.2024.31.1.1
36. Gupta, R.K., Anil Kumar, V., Christy Mathew, G. Sudarshan Rao (2016) Strain hardening of Titanium alloy Ti–6Al–4V sheets with prior heat treatment and cold working. *Materials Sc. and Eng*., **662**, 537–550. DOI: https://doi.org/10.1016/j.msea.2016.03.094

ORCID
V. Korzhyk: 0000-0001-9106-8593,
A. Grynyuk: 0000-0002-6088-7980,
O. Babych: 0000-0001-5633-5721,
O. Berdnikova: 0000-0001-9754-9478,
Ye. Illiashenko: 0000-0001-9876-0320,
O. Bushma: 0009-0005-6611-4507

CONFLICT OF INTEREST
The Authors declare no conflict of interest

CORRESPONDING AUTHOR
V. Korzhyk
E.O. Paton Electric Welding Institute of the NASU
11 Kazymyr Malevych Str., 03150, Kyiv, Ukraine.
E-mail: vnkorzhyk@gmail.com

SUGGESTED CITATION
V. Korzhyk, A. Grynyuk, O. Babych, O. Berdnikova, Ye. Illiashenko, O. Bushma (2025) Obtaining functionally-graded metal-matrix materials Ti–6Al–4V + WC in the process of 3D printing by the method of additive plasma-arc deposition. *The Paton Welding J*., **8**, 29–36.
DOI: https://doi.org/10.37434/tpwj2025.08.03

JOURNAL HOME PAGE
https://patonpublishinghouse.com/eng/journals/tpwj

Received: 13.05.2025
Received in revised form: 18.06.2025
Accepted: 07.08.2025